Non-linear growth of periodic patterns

Simon Villain-Guillot

Centre de Physique Moléculaire Optique et Hertzienne,
Université Bordeaux I,
33406 Talence Cedex, France

Christophe Josserand

Laboratoire de Modélisation en Mécanique, UMR CNRS 7607
Université Pierre et Marie Curie, 8 rue du Capitaine Scott, 75015 Paris,
France

Abstract

We study the growth of a periodic pattern in one dimension for a model of spinodal decomposition, the Cahn-Hilliard equation. We particularly focus on the intermediate region, where the non-linearity cannot be negected anymore, and before the coalescence dominates. The dynamics is captured through the standard technique of a solubility condition performed over a particular family of quasi-static solutions. The main result is that the dynamics along this particular class of solutions can be expressed in terms of a simple ordinary differential equation. The density profile of the stationary regime found at the end of the non-linear growth is also well characterized. Numerical simulations correspond satisfactorily to the analytical results through three different methods and asymptotic dynamics are well recovered, even far from the region where the approximations hold.

1

I. INTRODUCTION

When a homogenous system departs suddenly from equilibrium, the fluctuations around the initial ground state are linearly amplified and for example the homogenous phase separates spontaneously into two different more stable states. The interfaces which delimit the domains of each phase form a complex pattern and interact with each other, giving rise to interface dynamics or pattern formation. Its results can be a slow process of coarsening which ends up with only two well separated domains. This process of first order phase transition arises particularly for binary mixtures [1] or alloys [6], vapor condensation [2], ferromagnetic Ising model [3] or thin films of copolymers [4].

For the most general, first order transitions initiate in two different ways: first, a nucleation process, where the homogenous state is put suddenly in a metastable configuration, and an energy barrier has to be crossed before the transition appears. This is the typical dynamics of cavitation, for instance [5]. The other method is spinodal decomposition where the system leads in a linearly unstable configuration; such is the situation that we will study here. In this latter case, three different regimes are identified in the dynamics: first the linear instability of the homogenous phase develops from the fluctuations, leading to the creation of a modulation of the order parameter at a well defined length scale. The modulations grow exponentially with time as long as the non-linearities are negligeable. This stage is very short and results mainly in the selection of a particular length scale for the process. Non-linearities rapidly slow down the growth of the modulation resulting in an interface pattern composed of well defined interfaces delimiting domains containing one of the two stable phases. Remarkably, this intermediate stage conserves quite perfectly the modulation width, so that the resulting pattern is of almost the same length scale than the one selected initially. Finally, a slow, self-inhibiting dynamics dominates the last stage of the process, due to the interactions between the interfaces. The different regions of each phase coalesce in the so-called Ostwald ripening where the number of domains diminishes whereas their typical size increases. The asymptotic state is decomposed into two domains, one for each phase. This coarsening dynamics is in fact present already from the beginning of the spinodal decomposition; however, as we will discuss below, its influence on the two first stages can be often neglected.

Hillert [6], Cahn and Hilliard [7] have proposed a model equation for a scalar order parameter describing the segregation for a binary mixture. This model, known as the Cahn-Hilliard equation (C-H later on), belongs to the Model B class in Hohenberg and Halperin's classification [3]. Indeed, different models of phase separation have been proposed, depending whether the order parameter is a scalar or a vector, or wether it is or is not a conserved quantity (for a review see [3,8,9]). The (C-H) equation is in fact a standard model for phase transition with conserved quantities and has applications to phase transition in liquid crystals [10], segregation of granular mixtures in a rotating drum [11], or formation of sand ripples [12,13]. It is a partial differential equation to which a conservative noise is added to account for thermal fluctuations [14].

Figure (1) shows snapshots of the numerical simulation of the (C-H) dynamics which

represents the full phase transition process after a quench in temperature. In that case, thermal fluctuations have been omitted in the dynamics, but were present in the initial conditions. The three main stages of the spinodal decomposition described above are clearly distinguished: first, from Fig. (1 (a)) to Fig. (1 (b)), we observe the selection of a typical length scale for the modulations, then the non-linear growth and its saturation from Fig. (1 (b)) to Fig. (1 (c)). We note that the number of peaks has been almost conserved between these two configuration; on the other hand the amplitude of the modulation has now reached almost its asymptotic value and will not change significantly in the further dynamics. On the contrary, the coarsening dynamics is observed between Fig. (1 (c)) and Fig. (1 (d)) and the typical length of the pattern is increasing.
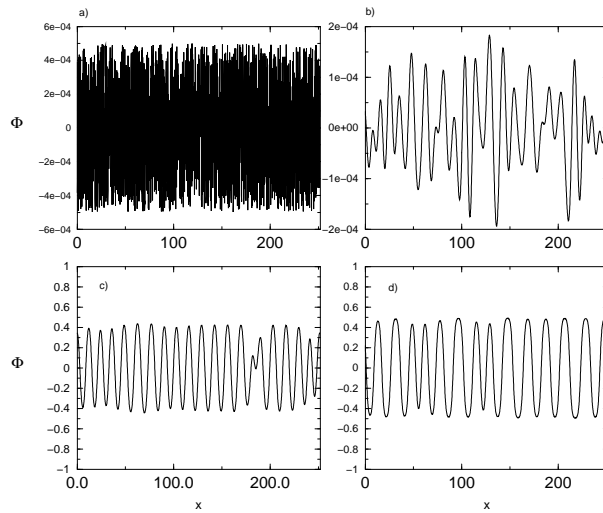
FIGURES

FIG. 1. Time evolution of the order parameter $\Phi(x,t)$ for $\varepsilon = -1$, $dx = 0.1227$. (a) initial conditions at $t = 0$ are taken randomly with a very low amplitude $(5 \cdot 10^{-4})$; (b) at time $t = 15$, the amplitude of the modulation has decreased, while only long wavelength contributions are still present. The small scale perturbations have been damped by the (C-H) dynamics ; (c) at $t = 225$, the modulation has almost reached its final amplitude, keeping roughly the same number of peaks as before ; (d) at $t = 1800$, we observe that the number of domains has decreased from the coarsening dynamics.

Note that in the numerical experiments, contrary to a realistic experience, we go instantaneously from one temperature to an other (ideal quench). And we will see in the following that the system will evolve in a smoother ways in the sense that, due to finite diffusion process, it will not instantaneously reach the thermodynamical state associated with the temperature of the quench.

In this paper, we will focus on the one dimensional (C-H) equation and our aim is to offer a consistent description for the pattern formation, corresponding to the intermediate (non-linear) regime. We will obtain a simple ordinary differential equation describing the dynamics along a family of quasi-static periodic solutions. We recover the linear regime for short times, and correctly reproduce the saturation of the second (non-linear) stage, in the case of small initial perturbations, in the region close to the critical point (i.e., for a symmetric mixture). These results are valid in the limit where thermal fluctuations and coarsening processes are both neglected. We will discuss these important assumptions and show how the resulting ordinary equation depends on the wavelength of the periodic solution.

As mentionned above, numerous models for phase transition have been proposed ; an important activity has been devoted to the description of their dynamics, using both statistical methods or numerical simulations (for a review see [15]). However, these works mainly concentrate on the late stage of the spinodal decomposition where the coarsening dynamics dominates and which exhibits "dynamical scaling" : the dynamics presents a self-similar evolution where time enters only through a length scale $L(t)$, associated with a typical length of the domains or the rate of decay of the inhomogeneities. For instance, scaling arguments

4

and stability criteria give the law $L(t) \sim t^{1/3}$ for spatial dimensions greater than one and a logarithmic behavior for one dimension in the case of the (C-H) equation [15].

In this article, by spinodal decomposition, we refer to the two first stage only, excluding the coarsening dynamics or the third stage.

Only little is known experimentally of these two regimes of the dynamics: indeed, they are too brief and therefore very hard to capture. However, these stages were observed in a recent experiment on two-dimensional demixion of copolymer [4] which motivated our work since it shows the need for a better understanding of the dynamics before the coalescence. While the linearized theory gives a full understanding of the first stage, the second stage of phase separation, which concerns the saturation of the growth through the non linearity, appears to have been less studied. There exists numerical attempts to provide descriptions of the saturation of the profile up to its stationary regime, using for example a concentration dependant diffusion coefficient, [16] $D = D_o\Phi(1 - \Phi)$, which leads to a modified Kuramoto-Shivashinski equation and enables to have a saturation of growth. Here, on the contrary, we work with a constant diffusion coefficient : the non-linearity will only come from the usual Φ^4 term of the Landau free energy.

The paper is organized as followed: first, we present a brief review of general properties of phase segregations and on the (C-H) model, mainly to fix the notation. We will reproduce briefly the original derivation by Cahn and Hilliard, and we will restrict ourselves to the one dimensional case. In part III, we motivate the different assumptions of our calculations. Numerical simulations are used to determine the role of the noise and the influence of the coarsening in the early dynamics. Then, in part IV we focus on interfaces ; in particular, we will exhibit a two parameters family of solutions, specific of the one dimensional case, the so-called soliton lattice. Finally in section V, we will make use of the solvability criterion in order to select the dynamical evolution of the density profile among a selected "ansatz" solution. Eventually, we compare these results with numerical studies of the full (C-H) dynamics shown at the end. We conclude with a discussion of possible extensions of this work.

II. THE CAHN-HILLIARD MODEL

The Cahn-Hilliard theory is a modified diffusion equation ; it is a continuous model, which reads in its dimensionless form:

$$\frac{\partial \Phi}{\partial t}(\mathbf{r}, t) = \nabla^2(\frac{\varepsilon}{2}\Phi + 2\Phi^3 - \nabla^2\Phi). \tag{1}$$

Here $\mathbf{r}$ and t represent the position vector and the time, the vectors being noted with bold fonts. Φ is the order parameter, a real number ; for instance, it can correspond to the dimensionless magnetization in Ising ferromagnet, to the fluctuation of density of a fluid around its mean value during a phase separation or to the concentration of one of the components of a binary solution in some region around $\mathbf{r}$. D is the diffusion constant and ε is the dimensionless control parameter of the system ; it is often identified to the reduced temperature ($\varepsilon = \frac{T-T_c}{T_c}$ where T_c is the critical temperature of the phase transition). This equation, first derived by Cahn and Hilliard [7], has also been retrieved by Langer [17] from microscopic considerations. As written, the (C-H) equation does not account

5

for thermal fluctuations present in the system. They can be added through a Langevin force, which integrates in the Fokker-Planck equation for the probability distribution of $\Phi(t)$ [17]. However, as explained by [7,14,9], the thermal fluctuations can equivalently be taken in account through a random noise term on the r.h.s. of equation (1). Thus, the (C-H) equation reads, in its more general form:

$$\frac{\partial \Phi}{\partial t}(\mathbf{r}, t) = \nabla^2(\frac{\varepsilon}{2}\Phi + 2\Phi^3 - \nabla^2\Phi + \zeta(\mathbf{r}, t)), \tag{2}$$

where ζ is a white noise of norm unity, whose amplitude is proportional to the square root of the temperature of the system.

The (C-H) model is a conservative model for the order parameter Φ. Indeed, it can be written as:

$$\frac{\partial \Phi}{\partial t} = -\nabla \cdot \mathbf{j}$$

where $\mathbf{j}$ is the current associated with Φ. Moreover, this current obeys the standard law related to the gradient of a so-called chemical potential μ ($\mathbf{j} = -\nabla\mu$). For (C-H), μ is itself defined as the functional derivative of a free energy F, through:

$$\mu = \frac{\delta F}{\delta \Phi}$$

with F being in that case the usual Landau-Ginzburg density:

$$F = \frac{1}{2}\left((\nabla\Phi)^2 + \frac{\varepsilon}{2}\Phi^2 + \Phi^4\right)$$

The homogeneous stationary solutions for the noiseless (C-H) equation are extrema of the effective potential $V(\Phi) = \varepsilon\Phi^2 + \Phi^4$. For positive ε, there is only one homogenous solution $\Phi = 0$ which is linearly stable ; for negative ε, the stationary solution $\Phi = 0$ undergoes a pitchfork bifurcation and three stationary solutions exist. $\Phi = 0$ is still a stationary solution, but it is now linearly unstable ; two other symmetric solutions $\Phi = \pm\frac{\sqrt{-\varepsilon}}{2}$ are stable and have the same free energy $F = -\varepsilon^2/32$.

Thus, a first order transition can be experienced by quenching the system suddenly from a positive reduced temperature ε to a negative one. Spinodal decomposition is the resulting dynamics. Since for all positive ε the system is described by $\Phi = 0$, we only have to study the case where we start at $t = 0$ with $\Phi = 0$ and a negative ε. This is what was shown on figure (1) in one space dimension, where the noise has been omitted except for the initial condition, where it consists of a random noise of small amplitude around the mean value $< \Phi >= 0$. This can be justified since the noise level, being proportional to the square root of the temperature, is higher before the quench than after. Thus, taking a noisy initial condition and omitting the noise further on can be interpreted as neglecting the noise of the quenched system compared to the residual noise coming from the "hot" initial temperature. However we will discuss more precisely below the influence of the noise in the quenched phase.

When the equation is studied for a constant ε, via a rescaling of Φ (as $\sqrt{-\varepsilon}\Phi$), position $\mathbf{r}$ (as $\mathbf{r}/\sqrt{-\varepsilon}$) and time (as $t/|\varepsilon|^2$), we observe that we could restrict the dynamics to the case $\varepsilon = -1$. However, since we will later on compare stationary solutions of (C-H) with different reduced temperature, we will continue to write the equation with a given ε, keeping in mind that the dynamics can always be rescaled to the case $\varepsilon = -1$.

The stability of the solution $\Phi = 0$ can be studied by linearizing equation (1) around $\Phi = 0$ (i.e. neglecting the non linear term Φ^3); considering Φ as a sum of Fourier modes:

$$\Phi(\mathbf{r}, t) = \sum_{\mathbf{q}} \phi_{\mathbf{q}} e^{i\mathbf{q}\cdot\mathbf{r}+\sigma t}$$

where ϕ_q is the Fourier coefficient at $t = 0$, we obtain that the amplification factor $\sigma(q)$ satisfies:

$$\sigma(\mathbf{q}) = -(q^2 + \frac{\varepsilon}{2})q^2$$

It shows immediately that $\Phi = 0$ is linearly stable for $\varepsilon > 0$ while a band of Fourier modes are unstable for negative ε, since $\sigma(\mathbf{q}) > 0$ for $0 < q < \sqrt{(-\varepsilon/2)}$. Moreover, the most unstable mode (where σ is maximal) is for $q_m = \sqrt{-\varepsilon}/2$ (with $\sigma_m = \frac{\varepsilon^2}{16}$). We can anticipate that this wave number of maximum amplification factor will dominate the first stage of the dynamics; in particular, it explains why the modulations appear at length scales close to $\lambda_m = 2\pi/q_m$, the wave length associated with q_m. Indeed, we show on figure (2) the time evolution of the usual structure factor in one dimension:

$$S(q) = \hat{\Phi}(q)\hat{\Phi}(q)^*$$

where $\hat{\Phi}$ is the Fourier transform of the field Φ ($\hat{\Phi}^*$ standing for its complex conjugate). We have taken the noiseless (C-H) equation with random initial conditions; the curve is obtained through an average over 100 initial conditions.
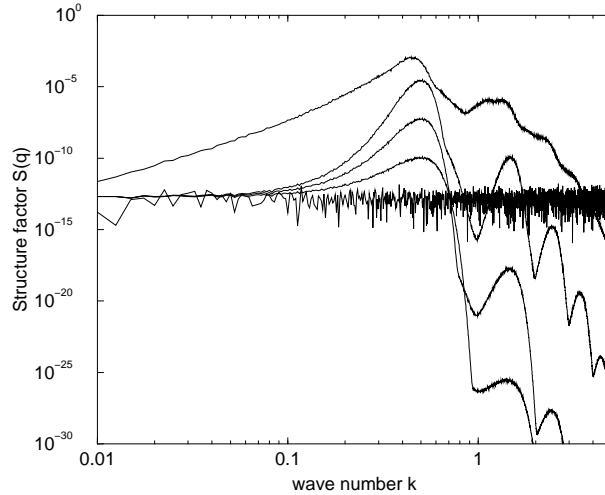
FIG. 2. The structure factor $S(q)$ as a function of the wave number q for different time $t = 0, 50, 100, 150$ and $t = 500$ time units; the higher the peaks are, the larger the time. The curves are an average over 100 initial conditions taken as a random noise of amplitude $5 \cdot 10^{-4}$, the discretization is over 4096 grid points with the grid space $dx = 0.6$, and $\varepsilon = -1$. At $t = 0$, we observe the flat spectrum of the white noise. For $t = 50$, the spectrum reflects the amplification fator: the peaks of the factor is located at $q_m = 0.5$ while for all the modes $q > \sqrt{2}$ the initial noise has been damped. Then for $t = 100$ and $t = 150$ we observe the formation of higher harmonics but the peaks of the structure factor stay around q_m. However, at $t = 500$. the coarsening of the solution has began since the maximum of $S(q)$ is now at a larger wave length.

The different regimes are again well identified: at short times we see that the modulations whose wave number is close to q_m grow rapidly from the white noise, while the fluctuations for $q > \sqrt{2}q_m$ for which the amplification factor is negative are damped. Then, higher wave numbers emerge, which correspond roughly to harmonics mode of the initial modulations. It corresponds to the intermediate stage of the dynamics, where the single mode approximation of the profiles is not valid any more and the dynamics is in a highly non-linear regime. Notice however that the structure factor keeps its peak located around q_m; as we will discuss below, it is indicating that the number of domains stays almost unchanged during this regime. Later on, interfaces separating each domain are formed and interact only through coalescence dynamics: $S(q)$ changes slowly through a self-similar process (see [17]) and the peak of the function will slowly move to smaller wave numbers.

III. AN ADIABATIC ANSATZ

Our analytic method will rely on the assumption that the intermediate region is approximated through the growth of a periodic modulation solution of the noiseless (C-H) equation: we need therefore to discuss how this approach is relevant to the general case where noise is present and where the coarsening of the non-periodic pattern acts. Indeed, as it can be seen on figure (2), the coalescence, roughly characterized by the evolution of the position of the peak of the structure function, does not appear to influence the dynamics before a few hundreds of units time. At those times, the intermediate regime has ended and the modulated pattern is formed. More precisely, figure (3) shows the typical mean width of the pattern as a function of time for the same conditions as figure (2); after a transient behavior (until about $t = 50$) where the size of the pattern is dominated by the initial conditions combined with the linear theory of (C-H), we observe the intermediate regime (for t between 50 and 200 roughly). In particular, for this regime, we note that the average size of the modulation is λ_m, with a deviation of less than one percent from the value predicted by the linear theory. It does not mean that each modulation has a length scale of λ_m, but more precisely that the distribution of the modulations length is centered around λ_m, as can be seen from the structure factor (see figure (2)). Moreover, it suggests that the growth of each modulation is achieved at constant length scale, determined by the initial linear instability and thus centered around λ_m. At t around 200, the growth of the modulation is saturate (as can be seen from figure (1)) and the coalescence dominates the future dynamics : the length scale of the structures slightly increases with time. The inset of figure (3) shows equivalently the

8

typical wave length of the modulations for the (CH) model in two spatial dimensions; it shows again the same plateau that is in favor of the pattern growth at a constant size.
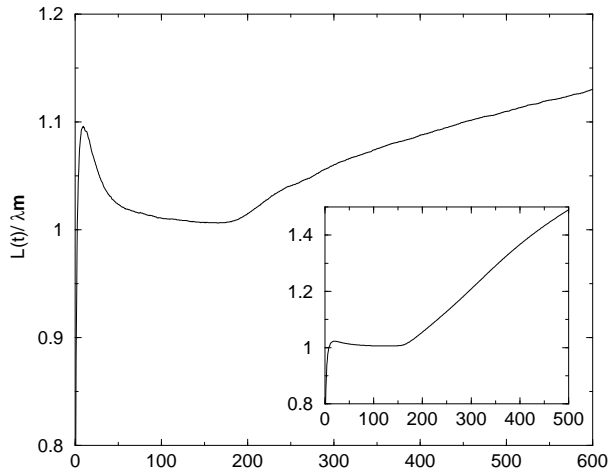

FIG. 3. The ratio between the mean length of the modulations and the most amplified wavelength $\lambda_m = 2\pi/q_m$ as a function of time, for the same conditions than figure (2). The inset shows a similar curve in two space dimensions, obtained by computing the mean wave number as a function of time, over ten initial conditions.

Thus, we have shown that the coalescence due to the non-periodic pattern selected at short time can be neglected during the growth of the modulations. We need also to quantify the influence of the noise during the dynamics: until now, we have simplified it to the initial conditions which induce then a non-periodic initial pattern which is sufficient to characterize the general features of the spinodal decomposition. Moreover, we have shown that the growth of the modulation during the intermediate regime can be considered to occur at constant length (centered around λ_m) for each modulation. But strictly speaking, noise is always present in the dynamics and, in addition to feeding the linear instability of the homogenous solution ($\Phi = 0$) for short time, it generates a systematic seed of perturbations to the quasi-periodic pattern. It can therefore disturb this apparent frozen dynamics at constant size. Figure (4) characterizes its effect through the evolution of the mean length of the modulation for different noise levels. Each curve presents the same behavior, transient dynamics which selects a length scale of the order of λ_m, then a plateau regime (beginning around $t = 50$), which corresponds to the non linear growth, followed by a coalescence dynamics. We observe that the length of the plateau regime, on which we are focusing, depends strongly on the noise level. In particular, for low noise levels, the growth of the modulation seems to occur at the constant length λ_m, during a long period after $t = 50$. But, the higher the noise level, the shorter is this plateau. The noise stimulates the coalescence process, which interferes more with the pattern during the intermediate regime [2]. For noise levels higher than 10^{-4}, the growth regime cannot be differentiated anymore from the coalescence dynamics and in such cases, our assumption of growth at a constant scale would no longer be valid.
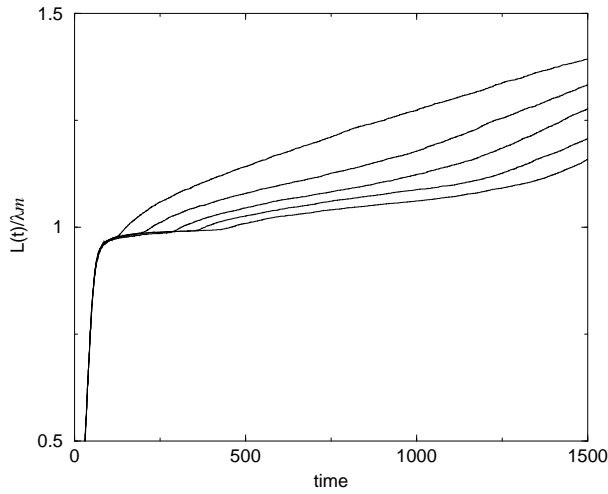
FIG. 4. The ratio between the mean length of the modulations and the most amplified wavelength $\lambda_m = 2\pi/q_m$ as a function of time, for different noise level, from 10^{-10} to 10^{-2} (the noise being multiplied by 100 between each curve). The shorter the nonlinear plateau, the higher the noise level. Each curve is obtained through an average over 100 runs. The other characteristics of the simulations are the same as for figure (3).

In conclusion, we can consider that, for low enough noise level, the non linear growth of the modulations is made at constant length scale and that the noise has a very weak influence on the dynamics of the two first stages.

Taking advantage of this observation, we can simplify the particular study of the second stage of the dynamics, the non-linear saturation. The aim of this paper is therefore to present a detailed calculation for the growth of a periodic modulation of constant size, for the noiseless (C-H) equation (1) in one spatial dimension for a fixed temperature ε_0.

However we hope that this approach is valid also in the limit of the small noise levels, where the growth of each modulation appears to be unperturbed. Although the numerical comparison is developed for the particular case of λ_m periodicity, it applies to any wave length.

We can now use known results concerning non-homogeneous solutions of the Ginzburg-Landau equation.

IV. QUASI-STATIC APPROXIMATION

In order to describe our method, we will first describe a particular family of stationary solutions of the one dimensional (C-H).

For $\varepsilon < 0$, a stationary solution exists that relies the two homogenous phases $\Phi = \pm\frac{\sqrt{-\varepsilon}}{2}$

$$\Phi(x) = \frac{\sqrt{|\varepsilon|}}{2} \tanh(\frac{2x}{\sqrt{|\varepsilon|}}). \tag{3}$$

Such a monotonic solution allows a continuum description of the interface between the two stable phases. In fact, this is a particular member of a one parameter family of stationary solutions of the Ginzburg-Landau equation

10

$$\frac{\varepsilon}{2}\Phi + 2\Phi^3 - \nabla^2\Phi = 0 \tag{4}$$

These solutions, the so-called soliton-lattice solutions [18], are :

$$\Phi_{k,\varepsilon}(x) = k\Delta\mathrm{Sn}(\frac{x}{\xi}, k) \text{ with } \xi = \frac{1}{\Delta} = \sqrt{2\frac{k^2+1}{-\varepsilon}} \tag{5}$$

where $\mathrm{Sn}(x, k)$ is the Jacobian elliptic function sine-amplitude. This family of solutions is parametrized by ε and the modulus $k \in [0, 1]$. These solutions describe a periodic pattern of period

$$\lambda = 4K(k)\xi, \text{ where } K(k) = \int_0^{\frac{\pi}{2}} \frac{\mathrm{d}t}{\sqrt{1 - k^2 \sin^2 t}} \tag{6}$$

is the complete Jacobian elliptic integral of the first kind. This family of profiles (or alternating interfaces) can be obtain exactly as a periodic sum of single solitons and antisolitons (or alternating interfaces) [18]

$$\sum_n (-1)^n \tanh(\pi s(x - n)) = \frac{2k(s)K(s)}{\pi s}\mathrm{Sn}(x, k) \text{ with } s = \frac{K(k)}{K(k')} \text{ and } k'^2 = 1 - k^2$$

The soliton-lattice solution can be associated with a micro phase separation locally limited by the finite diffusion coefficient. For $k = 1$, $\mathrm{Sn}(x, 1) = \tanh(x)$, we recover the usual interface solution ; it is associated with a one soliton solution and corresponds to a macroscopic segregation. Note that $K(1)$ diverges ; the solution

$$\Phi_{1,\varepsilon}(x) = \frac{\sqrt{|\varepsilon|}}{2}\tanh(\frac{\sqrt{|\varepsilon|}}{2}x).$$

is thus the limit of infinite s, when the solitons are far apart one each others (strong segregation regime).

In the opposite limit ($k \to 0$, or weak segregation regime) it describes a sinusoidal modulation

$$\lim_{k\to 0}\Phi_{k,\varepsilon}(x) = k\sqrt{\frac{|\varepsilon|}{2}}\sin(\sqrt{\frac{|\varepsilon|}{2}}x)$$

We now seek the evolution of the solution $\Phi(x, t)$, according to the (C-H) noiseless dynamics, for a fixed reduced temperature ε_0:

$$\frac{\partial\Phi}{\partial t}(x, t) = \partial_{xx}(\frac{\varepsilon_0}{2}\Phi + 2\Phi^3 - \partial_{xx}\Phi), \tag{7}$$

Numerical simulations of that problem with a small initial condition of periodicity λ, shows the growth of the modulation at this periodicity λ. As discussed in the previous section, such dynamics is unstable and would, in the presence of noise for instance, loose its periodicity. However, we have shown that this can be neglected for low enough noise levels, and that this "unstable" growth of the pattern is relevant there.

The initial condition will then be taken as the sine mode $q = \frac{2\pi}{\lambda}$:

11

$$\Phi(x, t = 0) = \nu \sin(q_{max} x)$$

where ν is an arbitrary small amplitude. This profile is a member of the soliton-lattice family (for very small k).

The core of the method we are using involves tracking the evolution of the periodic modulations through a simplified equation. For that purpose, we now make the *ansatz* that at first order, these modulations belong at any time to the two parameters family of solutions Φ_{k,ε^*}, with k and ε^* being functions of time. Since the period is chosen to be constant and equal to λ, using equations (5) and (6), we find that k and ε^* are related to one another through

$$\varepsilon^*(k) = -2(1 + k^2) \left(\frac{4K}{\lambda}\right)^2. \tag{8}$$

and we have eventually selected a one parameter sub-family of solutions of given spatial periodicity (that we will call $\Psi^*(x, k)$ later on) :

$$\Psi^*(x, k) = \frac{4K(k) \cdot k}{\lambda} \text{Sn}\left(\frac{4K(k)x}{\lambda}, k\right).$$

The dynamics of $\Phi(x, t)$ is now reduced to the evolution of $k(t)$ (or equivalently $\varepsilon^*(t)$). Given a function Φ (obtained either from experimental data or numerical simulation of equation (7)) at time t, the *ansatz* assumes that there exists k so that $\Phi(x, t) \sim \Psi^*(x, k)$. $\varepsilon^*(t)$ can be then interpreted as a fictitious temperature : it is the temperature extracted from the profile at a given time, using the correspondence between ε^* and k of equation (8). For instance, at $t = 0$, the amplitude is small and we find that $k(0) = \frac{\nu \lambda_m}{2\pi}$ and thus $\varepsilon^*(0) = 8\pi^2/\lambda^2$, different *a priori* from ε_0 ($\varepsilon^*(0) = \frac{\varepsilon_0}{2}$ in the limit $\nu \to 0$, for $\lambda = \lambda_m$). In the same spirit, we expect that at the end of the growth, the "local temperature" of the interface coincides with the thermodynamic one, i.e. the quench temperature ε_0

$$\lim_{t \to \infty} \varepsilon^*(t) = \varepsilon_0$$

at which the dynmics ends. Somehow, we have assumed that the dynamics of (C-H) can be projected at first order onto a dynamics along the sub-family $\Psi^*(x, k)$, which can be considered as an attractor of the solutions. This is well justified when a non sinusoidal initial condition (of small amplitude) is chosen: we then observe, in numerical simulations, a short transient in the dynamics which drives the solution towards the sine mode at roughly the same amplitude. However, for consistency, we need to check that at any time, the solution of (C-H) can be well approximated by a member of the sub-family. For this purpose, we have developed three different algorithms, taking advantage of the general properties of the family of solutions $\Phi_{k,\varepsilon}$: either, k can be deduced both from the amplitude of the oscillation equals to $4kK(k)/\lambda$, or from the relation $k = 1 - \left((\Phi(\lambda/2, t)/\Phi(\lambda/4, t))^2 - 1\right)^2$; thirdly, a straightforward computation relates k to the ratio of the two first terms of the Fourier transform of Φ. We have observed that the three methods show in general similar results within an error of one percent. However, the validity of the ansatz has still to be checked by comparing the initial function $\Phi(x, t)$ with the extrapolated function $\Psi^*(x, k)$ obtained by one of these three procedures. It is shown in figure (5) at two different times

in a numerical simulation of (7) ; we observed that the relative differences between the two function is much less than 0.01.
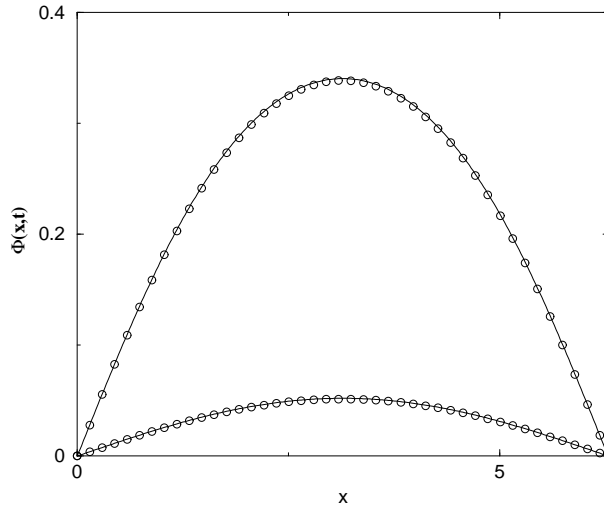

FIG. 5. Comparison for time $t = 100$ and $t = 140$ between the numerical solution of (7) (circles) and the functions $\Psi^*(x,k)$, with k extrapolated from the Fourier transform of $\Phi(x,t)$. Initial conditions are taken with $\nu = 10^{-4}$, and $\lambda = 2\pi/q_m$

Moreover, a zoom on the very early time of the one dimensional numerical simulation with small sinusoidal initial conditions, as presented in figure (6), shows a discrepancy between the different methods used to extract k from the numerics. In fact using the ratio between the Fourier series coefficients or the ratio between the amplitude at two specific points of the profiles, gives for the very beginning of the numerical simulation the value $k = 0$, in agreement with the statement of the initial condition[1]. Indeed, these two methods account for the shape of the profile, which has been taken initially as a sine mode, instead of a Sn mode.

However, the use the third method, which depends on the amplitude, leads to a small but finite $k = 0.02$ due to the small but finite value of ν. Even if the distortion from a sinusoidal function associated with this finite Jacobi modulus is small (the relative change in the natural period and in the shape of the function is of order 10^{-4}), one nevertheless observes that the dynamics of the system is such that, within a short time, the three methods give results which are again in agreement. There is a short inflation period during which there is a change in the shape of the profile and where the shoulders of the initial sinusoidal inflate. That is, there exist a very short stage during which the system goes very rapidly to a state very close to an element of the family of the soliton lattice $\Psi^*(x,k)$.

---

[1]Remark also that these two methods give estimations of k that are so close that they cannot be differenciated in figure (6).
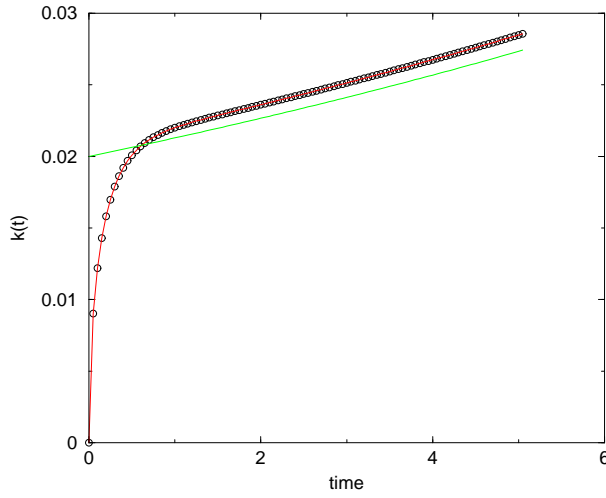
FIG. 6. Comparison for the very early times of the dynamics between the $k(t)$ predicted by the three different methods. The ratio between the Fourier series coefficients (circles) and the ratio between the amplitude at $\Phi(\lambda_m/2, t)$ and $\Phi(\lambda_m/4, t)$ (gray line) both start at $k = 0$ and almost coincide. On the contrary, the third method, which uses the amplitude of the profile, starts from a finite value. Nevertheless, the three methods merge within a short time, indicating the "affinity" of the (C-H) dynamics for soliton-lattice solutions.

V. NON-LINEAR GROWTH

Although the evolution of $k(t)$ can be extracted from direct numerical simulations of (7), as shown above, the aim of the rest of this work is to show that $k(t)$ can be deduced via an explicit ordinary differential equation. Therefore, in what follows, we will seek the solution of (7) in the form

$$\Phi(x,t) = \Psi^*(x, k(t)) + \eta\varphi(x,t) \tag{9}$$

where φ accounts for high order correction terms to Ψ^*, while the "ansatz" assumes that $\eta \ll 1$ (we consider ε_0 and λ_m of order 1).

To describe the evolution of the modulus $k(t)$, or equivalently the dynamics for $\varepsilon^*(t)$, we will use the so-called solubility condition technique. Substituting formula (9) in the Cahn-Hilliard equation (7), it gives the following dynamics

$$\frac{\partial \Phi}{\partial t}(x,t) = \frac{\partial \Psi^*}{\partial k} \cdot \frac{\mathrm{d}k}{\mathrm{d}t} + \eta\frac{\partial}{\partial t}\varphi = \frac{\partial^2}{\partial x^2}\left(\frac{\varepsilon_0}{2}\Psi^* + 2\Psi^{*3} - \nabla^2\Psi^* + \eta\left(\frac{\varepsilon_0}{2}\varphi + 6\Psi^{*2}\varphi - \nabla^2\varphi\right)\right).$$

where we have kept only the lowest order terms in the perturbation. As $\Psi^*(x, k(t))$ satisfies the relation :

$$\varepsilon^*(k)\Psi^* + 4\Psi^{*3} - 2\nabla^2\Psi^* = 0,$$

we then have the following dynamics :

$$\frac{\partial \Psi^*}{\partial k} \cdot \frac{\mathrm{d}k}{\mathrm{d}t} + \frac{(\varepsilon^* - \varepsilon_0)}{2}\frac{\partial^2\Psi^*}{\partial x^2} + \eta\frac{\partial}{\partial t}\varphi = \eta\frac{\partial^2}{\partial x^2}(\frac{\varepsilon_0}{2}\varphi + 6\Psi^{*2}\varphi - \nabla^2\varphi)$$

14

The balance of the different terms gives the small parameter of the expansion $\eta \sim \varepsilon^* - \varepsilon_0$; we obtain $\frac{dk}{dt} \sim \eta$ and $\partial_t \varphi \sim \eta\varphi$. Neglecting the terms of order η^2 in the previous equation, we end up solving the linear system :

$$\frac{\partial^2}{\partial x^2}(\mathcal{L}\varphi) = \frac{\partial \Psi^*}{\partial k} \cdot \frac{dk}{dt} + (\varepsilon^* - \varepsilon_0)\frac{\partial^2}{\partial x^2}\Psi^*.$$

Here, $\mathcal{L}$ is the linearized C-H operator $\mathcal{L}\varphi = \eta\left(\frac{\varepsilon^*}{2} + 6\Psi^{*2} - \nabla^2\right)\varphi$. Strictly speaking, this analysis is valid only for $\varepsilon^* \sim \varepsilon_0$; however, it is a classical assumption of the solubility condition (confirmed below by the numerical results presented on figure (7)) to expand it for the whole dynamics.

A necessary condition for solution is that the right hand side of the system is orthogonal to the kernel of the adjoint operator $(\partial_{x^2}\mathcal{L})^\dagger$. The Goldstone mode $\partial_k \Phi_{k,\varepsilon^*}$, for $\varepsilon = \varepsilon^* = $const, is clearly an element of $\text{Ker}(\mathcal{L}^\dagger)$, and if we consider the distribution $\chi(x,t)$, such that $\frac{\partial^2}{\partial x^2}\chi(x,t) = \Phi_{k,\varepsilon^*}(x)$, then we have $\partial_k \chi \in \text{Ker}((\partial_{x^2}\mathcal{L})^\dagger)$ [2]. Thus, using the scalar products $<|>$ over the period λ, defined as

$$< f|g > = \frac{1}{\lambda} \int_{-\lambda/2}^{\lambda/2} f(x)g(x)dx$$

we obtain the desired equation for $\frac{dk}{dt}$:

$$< \partial_k \chi \mid \partial_k \Psi^* > \frac{dk}{dt} = \frac{(\varepsilon_0 - \varepsilon^*)}{2} < \partial_k \chi \mid \partial_{x^2}\Phi_{k,\varepsilon^*} > = 4(\varepsilon_0 - \varepsilon^*)\frac{kK(k)}{\lambda^2(1+k^2)}\left(\frac{2E(k)}{1-k^2} - K(k)\right),$$

$$(10)$$

where $E(k) = \int_0^{\frac{\pi}{2}} \sqrt{1 - k^2\sin^2 x}\,dx$ is the complete Jacobi elliptic integral of the second kind. The l.h.s can be expressed using $\psi(x,t)$, defined as $\frac{\partial}{\partial x}\psi = \Psi^*$, which reads :

$$\psi(x,t) = \ln\left(\text{Dn}(\frac{x}{\xi},k) - k\text{Cn}(\frac{x}{\xi},k)\right) - \frac{1}{2}\ln(1-k^2).$$

Cn and Dn are the Jacobi elliptic function cosine and delta amplitudes respectively. Then, noting that

$$< \partial_k \chi \mid \partial_k \Psi_{k,\varepsilon^*} > = - < \partial_k \psi \mid \partial_k \psi > = -I(k)$$

where $I(k)$ is independent of λ. Finally, equation (10) can be recast as the following explicit ordinary differential equation for $k(t)$:

$$\frac{dk}{dt} = -4\left(\varepsilon_0 + 2(1+k^2)\left(\frac{4K(k)}{\lambda}\right)^2\right)\frac{kK(k)}{\lambda^2 I(k)(1+k^2)}\left(\frac{2E(k)}{1-k^2} - K(k)\right) \qquad (11)$$

---

[2]Remark that the partial derivative with respect to k is made with ε^* taken constant, since we are interested in a member of $\text{Ker}(\mathcal{L}^\dagger)$, linearized (C-H) operator for ε^*.

In the limit $k \to 0$, that is, for early times, equation (11) becomes, with the wave number $q = 2\pi/\lambda$ associated to the period λ

$$\frac{\mathrm{d}k}{\mathrm{d}t} = -q^2 (\frac{\varepsilon_0}{2} + q^2) \cdot k = \sigma(q)k.$$

Since k is proportional to the amplitude of the sine mode of wave number q, we observe that we retrieve the linear theory of (C-H) in that limit.

The r.h.s. of (11) is in fact proportional to $\varepsilon_0 - \varepsilon^*$, so that the dynamics ends when the fictitious temperature reaches the thermodynamic one ε_0; this occurs for $k = k_s$ which satisfies $32(1 + k_s^2)K(k_s)^2 = -\varepsilon_0\lambda^2$. For $\lambda = \lambda_m$, we obtain $k_s^2 = 0.471941$. This corresponds to the end of the non-linear growth (on figure (1 c))) and the value of k_s associated with this steady state is well retrieved numerically by the three methods explained above. Thus, the asymptotic steady state solution of equation (7) for a given period is $\lim_{t\to\infty} \Phi(x,t) = \Psi^*(x, k_s)$. However, no analytic solutions of equation (11) have been found, and we need to solve it numerically. Figure (7) compares the solution of (11) with the dynamic of k extracted by the Fourier method from the full (C-H) evolution, for the period $\lambda = \lambda_m$, the fastest growing mode. It shows a good agreement between the two curves; in particular, both limit $t \to 0$ and $t \to \infty$ are well captured ; thus equation (11) remains valid even for k far from k_s.
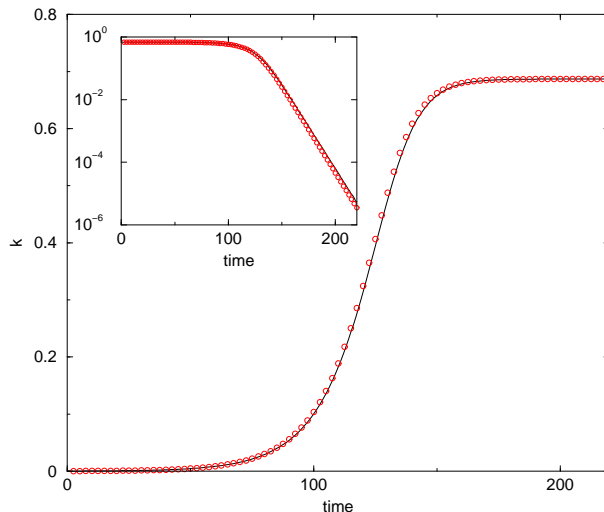

FIG. 7. Comparison between the solution of the ordinary differential equation (11) for the modulus $k(t)$ (black line) and the modulus extracted from the full (C-H) dynamics (circles) with the same initial condition $k(0) = 2 \cdot 10^{-4}$, for $\lambda = \lambda_m$. The dynamics converges to k_s in both case for large time. The inset shows the exponential convergence of both curves in asymptotic regime, where the solubility condition is valid ; it compares well with $k_s - k(t) \sim e^{-\varepsilon_0^2 t/8}$; in addition, far from k_s, the exponential growth for small time $k(t) \sim e^{-\varepsilon_0^2 t/16}$ is also retrieved by equation (11).

VI. CONCLUSION

We have shown that the choice of an ansatz within the soliton-lattice family allows a reliable description of the growth of a periodic pattern in the noiseless Cahn-Hilliard equation. Contrary to Ref. [19], our ansatz relies on the hypothesis that during the first

two stages of the dynamics, the periodicity of the order parameter remains constant. In this sense, it is an adiabatic ansatz. The validity of these assumptions has been investigated in detail and checked numerically (see Fig. 5). It enables to model the non-linear growth starting with spatial random initial conditions and predicts the stationary profile $\Psi^*_{k_s}$, which ends this non-linear growth. Although this profile might not be observable in a usual phase transition due to the presence of noise [17], we claim that this approach should be valid when the noise is low enough, which is the case when the quench is achieved at low temperatures. We expect this approach to have a particular pertinence for axial segregation in rotating drums [20], where the dynamics ends after the second stage.

The use of the solubility technique combined with the choice of an adiabatic ansatz might be generalized to the study of other non linear dynamics. For instance, spinodal decomposition in superfluid Helium or Bose condensate has been argued to be described by a cubic-quintic non linear equation [21] ; in this particular case, one would first need to retrieve a relevant soliton-like family of solutions along which to compute the adiabatic dynamics. The same difficulties would arise when the method is adapted to higher space dimensions.

Finally, this approach could be used to explore the self-similar scenario for coalescence suggested by AFM experiments for spinodal decomposition in mixtures of block co-polymers, depicted in Ref. [4], starting with the previous stationary distribution as initial conditions. The only change will be in the use of a family of solutions of growing periodicity λ_t, which would also be a slow variable of the position, since the coalescence is controlled by local interactions of the pattern [22]. The goal in that case would be to obtain a differential equation for λ the order parameter with the same technique. However, these questions are postponed to future studies.

REFERENCES

[1] C. Wagner, Z. Electrochem. **65**, 581 (1961).

[2] J.S. Langer, in *Solids Far From Equilibrium*, edited by C. Godrèche (Cambridge University Press, Cambridge, England 1992), pp. 297-363.

[3] P.C. Hohenberg and B.I. Halperin, *Rev. Mod. Phys.* **49**, 435 (1977).

[4] S. Joly, A. Raquois, F. Paris, B. Hamdoun, L. Auvray, D. Ausserre and Y. Gallot, *Phys. Rev. Lett.* **77**, 4394 (1996).

[5] S. Balibar, C. Guthmann, H. Lambaré, P. Roche, E. Rolley and H.J. Marris, *J. Low Temp. Phys.* **101**, 271 (1995).

[6] M. Hillert, *Acta Met.* **9**, 525 (1961).

[7] J.W. Cahn and J.E. Hilliard, *J. Chem. Phys.* **28**, 258 (1958).

[8] M.C. Cross and P.C. Hohenberg, *Rev. Mod. Phys.* **65**, 851 (1993).

[9] J.D. Gunton, M. San Miguel and P.S. Sahni, in *Phase Transition and Critical Phenomena*, edited by C. Domb and J.L. Lebowitz (Academic, London, 1983), Vol. 8, p. 267.

[10] C. Chevallard, M. Clerc, P. Coullet and J.M. Gilli, Eur. Phys. J. E **1**, 179 (2000).

[11] S. Puri and H. Hayakawa, cond-mat/9901260.

[12] M.A. Scherer, F. Melo and M. Marder, Phys. Fluids **11**, 58 (1999).

[13] A. Stegner and J.E. Wesfreid, Phys. Rev. E **60**, R3487 (1999).

[14] H.E. Cook, *Acta Met.* **18**, 297 (1970).

[15] I.M. Lifshitz and V.V. Slyozov, J. Phys. Chem. Solids **19**, 35 (1961). A.J. Bray, Adv. Phys. **43**, 357 (1994).

[16] A. Novik-Cohen and L.A. Segel, *Physica D* **10**, 277 (1984). R. Mauri, R. Shinnar and G. Triantafyllou, Phys. Rev. E **53**, 2613 (1996).

[17] J.S. Langer, Annals of Physics **65**, 53 (1971).

[18] A.I Buzdin and V.V. Tugushev, Sov. Phys. JETP **58**, 428 (1983). A. Saxena and A.R. Bishop, *Phys. Rev. A* **44**, R2251 (1991).

[19] J.S. Langer, M. Bar-on and H.D. Miller, *Phys. Rev. A*, **11**, 1417 (1975).

[20] Y. Oyama, *Bull. Inst. Phys. Chem. Res. Rep.* **5**, 600 (1939).

[21] C. Josserand and S. Rica, *Phys. Rev. Lett.* **78**, 1215 (1997).

[22] A.A. Fraerman, A.S. Mel'nikov, I.M. Nefedov, I.A. Shereshevskii and A.V. Shpiro, *Phys. Rev. B* **55**, 6316 (1997).